Acta Crystallographica Section F
Structural Biology and Crystallization Communications
ISSN 1744-3091

Crystallization and preliminary structural characterization of the two actin-depolymerization factors of the malaria parasite

Jani Huttu,[a,b]‡ Bishal Kumar Singh,[b]‡ Saligram Prabhakar Bhargav,[b] Julia M. Sattler,[c] Herwig Schüler[c]§ and Inari Kursula[a,b]*

[a]Centre for Structural Systems Biology, Helmholtz Centre for Infection Research and University of Hamburg, DESY, 22607 Hamburg, Germany, [b]Department of Biochemistry, University of Oulu, 90014 Oulu, Finland, and [c]Department of Infectious Diseases/Parasitology, Medical Faculty, Heidelberg University, 69120 Heidelberg, Germany

‡ These authors contributed equally to the work.
§ Current address: Structural Genomics Consortium, Karolinska Institute, 17177 Stockholm, Sweden.

Correspondence e-mail: inari.kursula@helmholtz-hzi.de

Received 10 March 2010
Accepted 26 March 2010

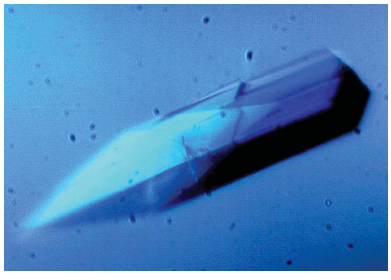

The malaria parasite *Plasmodium* depends on its actin-based motor system for motility and host-cell invasion. Actin-depolymerization factors are important regulatory proteins that affect the rate of actin turnover. *Plasmodium* has two actin-depolymerization factors which seem to have different functions and display low sequence homology to the higher eukaryotic family members. *Plasmodium* actin-depolymerization factors 1 and 2 have been crystallized. The crystals diffracted X-rays to maximum resolutions of 2.0 and 2.1 Å and belonged to space groups $P3_121$ or $P3_221$, with unit-cell parameters $a = b = 68.8$, $c = 76.0$ Å, and $P2_12_12$, with unit-cell parameters $a = 111.6$, $b = 57.9$, $c = 40.5$ Å, respectively, indicating the presence of one or two molecules per asymmetric unit in both cases.

1. Introduction

Malaria is one of the most devastating health threats to mankind and particularly affects developing countries in (sub)tropical regions. Malaria is caused by apicomplexan parasites of the genus *Plasmodium*. These parasites utilize a unique actin-based motor system for gliding motility and host-cell invasion (Sibley, 2004). Rapid polymerization and depolymerization of actin, which is regulated by a rather small set of actin filament-binding and monomer-binding proteins, is a prerequisite for movement of the parasite (Schüler & Matuschewski, 2006). *Plasmodium* actin filaments are extremely short and are located between the plasma membrane and the inner membrane complex of the parasite (Schatten *et al.*, 2003; Schmitz *et al.*, 2005). They are linked to host-cell surface receptors by a transmembrane protein complex, TRAP-aldolase (Jewett & Sibley, 2003), and to an array of unconventional myosins immobilized in the inner membrane complex (Bergman *et al.*, 2003).

Actin-depolymerization factors (ADFs) belong to the ADF/cofilin family, which comprises a group of important regulators of actin-filament dynamics (van Troys *et al.*, 2008; Bernstein & Bamburg, 2010). On the one hand ADFs bind to the side of actin filaments, thereby destabilizing the monomer–monomer interactions within the filament and leading to accelerated depolymerization rates. On the other they bind to ADP-bound actin monomers, inhibiting nucleotide exchange to ATP and thereby decreasing the rate of polymerization (Carlier *et al.*, 1997; Bamburg, 1999; Paavilainen *et al.*, 2008). At least two of the apicomplexan ADFs have been shown to be unable to bind to actin filaments (Schüler *et al.*, 2005; Mehta & Sibley, 2010). Unlike other Apicomplexa, *Plasmodium* species have two ADFs. Of these, ADF1 is similar to the ADFs present in other parasites of this class, while ADF2 more closely resembles conventional ADFs at the sequence level (Schüler *et al.*, 2005).

Because of constantly increasing drug resistance and the lack of an effective vaccination against malaria, there is an enormous need for new targets for drug or vaccine development. The actin cytoskeleton of the malaria parasite is an attractive target for pharmaceutical design because it is essential for the survival of the parasite and the invasion of host cells and is also significantly different from the

cytoskeleton of higher eukaryotes at the protein level. Here, we describe the expression, purification, crystallization and preliminary structural characterization of *P. falciparum* ADF1 (*Pf*ADF1; gi:23613057; PlasmoDB PFE0165w) and *P. berghei* ADF2 (*Pb*ADF2; gi:68159351; PlasmoDB PB001373).

2. Materials and methods

2.1. Cloning, expression and purification of the proteins

The coding regions of *Pf*ADF1 and *Pb*ADF2 were amplified by PCR on total genomic DNA from *P. falciparum* and *P. berghei* using the following primers with *Bam*HI and *Xho*I sites at the 5′ and 3′ ends, respectively: *Pf*ADF1 forward, 5′-CGTGGATCCGGGGTCAAGG; reverse, 5′-CCGCTCGAGTGTGTTTAATATTATAGT; *Pb*ADF2 forward, 5′-AGTTGGATCCATGGTTTCAGGAG; reverse, 5′-AGGACTCGAGTTATGTGTTTAAAATAATAG. The PCR products were digested with the respective enzymes and ligated into the pGEX-6P-1 vector (GE Healthcare). The resulting constructs were verified by restriction digestion followed by sequencing. Recombinant glutathione *S*-transferase (GST)-*Pf*ADF1 was expressed in *Escherichia coli* BL21 (DE3) RIPL cells. Transformed cells were grown for 36 h at 291 K in 800 ml autoinduction medium (Studier, 2005) supplemented with 100 µg ml^{-1} ampicillin and 25 µg ml^{-1} chloramphenicol. After 24 h, an additional dose of 125 µg ml^{-1} ampicillin, 0.03% glucose, 0.13% lactose and 0.3% glycerol was added to the culture to maintain cell growth and plasmid stability. The cells were harvested by centrifugation at 277 K and 4000*g* for 40 min and frozen; they were subsequently resuspended in lysis buffer consisting of 20 m*M* Tris–HCl pH 8.5, 50 m*M* NaCl, 5% glycerol, 10 m*M* dithiothreitol (DTT) and disrupted by sonication. The fusion protein was bound to glutathione Sepharose (GE Healthcare) in gravity-flow columns and eluted using a buffer consisting of 20 m*M* Tris–HCl pH 8.5, 50 m*M* NaCl, 5% glycerol, 10 m*M* DTT, 10 m*M* reduced L-glutathione. The pooled fractions containing the fusion protein were dialyzed overnight against 20 m*M* 4-(2-hydroxyethyl)-1-piperazineethanesulfonic acid (HEPES) pH 7.1, 2.5 m*M* DTT, after which the N-terminal GST tag was cleaved using 4.5 µg ml^{-1} recombinant 3C protease for 24–36 h at 277 K. The cleaved *Pf*ADF1 contained five additional residues (GPLGS) before the N-terminal Met. GST and other remaining contaminants were bound to Q-Sepharose FF (GE Healthcare) and the unbound *Pf*ADF1 was concentrated; final purification was performed by size-exclusion chromatography using a HiLoad 16/60 Superdex 75 pg column (GE Healthcare) equilibrated with 20 m*M* 3-(*N*-morpholino)propanesulfonic acid (MOPS) pH 6.5, 50 m*M* NaCl, 5%(*v*/*v*) glycerol, 2 m*M* DTT.

Recombinant GST-*Pb*ADF2 protein was expressed in *E. coli* BL21 Codon Plus (DE3) Rosetta cells grown in Luria–Bertani medium (1% tryptone, 0.5% yeast extract, 1% NaCl). Expression was induced with 0.6 m*M* isopropyl β-D-1-thiogalactopyranoside for 12 h at 291 K. The bacteria were harvested by centrifugation at 277 K and 15 300*g* for 15 min and frozen. The frozen cells were resuspended in lysis buffer containing 50 m*M* NaCl, 10% glycerol, 10 m*M* Tris–HCl pH 8.0 supplemented with an EDTA-free protease-inhibitor cocktail (Roche Diagnostics GmbH) and disrupted by sonication. The fusion protein was bound to glutathione Sepharose (GE Healthcare) in a gravity-flow column, eluted using a buffer containing 300 m*M* NaCl, 10% glycerol, 5 m*M* DTT, 20 m*M* reduced L-glutathione, 10 m*M* Tris–HCl pH 8.0 and dialyzed overnight against the same buffer without glutathione. The GST tag was cleaved using 3.5 µg ml^{-1} recombinant 3C protease for 6–8 h at 277 K. *Pb*ADF2 also contained the sequence GPLGS before the N-terminal Met after cleavage. The final purification step was performed by size-exclusion chromatography in buffer consisting of 300 m*M* NaCl, 10% glycerol, 5 m*M* DTT and 10 m*M* Tris–HCl pH 8.0 using a HiLoad 16/60 Superdex 75 pg column (GE Healthcare). Pure *Pb*ADF2 was flash-frozen in liquid nitrogen and stored at 193 K.

2.2. Characterization of purified *Pf*ADF1 and *Pb*ADF2

The identity of the purified proteins was verified by tryptic peptide mapping using mass spectrometry at the Biocenter Oulu Proteomics Core Facility. Because *Pf*ADF1 had a tendency to form both soluble and insoluble aggregates after cleavage of the GST tag, a thermal shift assay (Ericsson *et al.*, 2006) using the FRET channel in a Bio-Rad CFX96 Real Time System and a C1000 Thermal Cycler was performed to determine the optimal buffer conditions for purification and crystallization. Several buffers with different pH values and salts were tested. Each well contained 40 µl buffer, 8 µg protein and 4 µl 12× Sypro Orange dye (Invitrogen) in a total volume of 48 µl. The samples were heated from 291 to 368 K at a rate of 1 K min^{-1} in 96-well PCR plates sealed with optical sealing tape.

Analytical gel filtration injecting 100 µg *Pf*ADF1 in 20 m*M* MOPS pH 6.5, 100 m*M* NaCl, 2 m*M* DTT at a flow rate of 0.2 ml min^{-1} onto a Superdex 75pg 10/300 GL column (GE Healthcare) combined inline with three-angle static and dynamic light-scattering detectors (Wyatt Technology) was performed to determine the oligomeric state and monodispersity of *Pf*ADF1.

Synchrotron-radiation circular-dichroism spectroscopy (SRCD) was used to assess the folding and secondary-structure content of *Pb*ADF2. For the measurements, two samples, one of freshly purified protein and the second of protein stored unfrozen on ice for two weeks, at a concentration of 1 mg ml^{-1} were dialyzed against 10 m*M* potassium phosphate buffer pH 7.7, 50 m*M* NaF, 10% glycerol. The SRCD spectra were measured on beamline 3m-NIM at BESSY, Berlin, Germany in a cuvette with a 0.01 cm path length at 298 K from 170 to 280 nm wavelength with a 1 nm interval, as described previously (Majava *et al.*, 2009).

Small-angle X-ray scattering (SAXS) data for *Pf*ADF1 were measured on the MAX-Lab I711 beamline using *Pf*ADF1 at a concentration of 4.0 mg ml^{-1} in 20 m*M* MOPS pH 6.5, 100 m*M* NaCl, 5%(*v*/*v*) glycerol, 2 m*M* DTT. SAXS data for *Pb*ADF2 were measured on EMBL/DESY beamline X33 using *Pb*ADF2 at a concentration of 5 mg ml^{-1} in 300 m*M* NaCl, 10% glycerol, 5 m*M* DTT and 10 m*M* Tris–HCl pH 8.0. The corresponding buffer was always used for a blank experiment. The data were analyzed using programs from the *ATSAS* package (Konarev *et al.*, 2006). Further processing of the data was performed using *PRIMUS* (Konarev *et al.*, 2003) by subtracting the scattering by the buffer and normalizing the scattering by the proteins to a concentration of 1 mg ml^{-1}. The molecular weights of *Pf*ADF1 and *Pb*ADF2 were estimated by comparing the forward scattering $I(0)$ with that of a standard solution of human calmodulin or mouse 2′,3′-cyclic nucleotide 3′-phosphodiesterase. The distance distributions were obtained using *GNOM* (Svergun, 1992) and further used for *ab initio* modelling in *DAMMIN* (Svergun, 1999). An averaged model was generated from several runs using programs from the *DAMAVER* package (Volkov & Svergun, 2003). An estimate of the molecular weight was also calculated based on the model volume compared with those of standard proteins.

2.3. Crystallization

For crystallization, purified *Pf*ADF1 and *Pb*ADF2 were concentrated in the final purification buffers (20 m*M* MOPS pH 6.5, 50 m*M*

NaCl, 5%(*v*/*v*) glycerol, 2 m*M* DTT for *Pf*ADF1 and 10 m*M* Tris–HCl pH 8.0, 300 m*M* NaCl, 10% glycerol, 5 m*M* DTT for *Pb*ADF2) to approximately 10 mg ml^{-1} using centrifugal concentrators with a molecular-weight cutoff of 5 kDa (Millipore). Crystallization screens were set up in MRC conical-bottom sitting-drop vapour-diffusion plates (Molecular Dimensions) both at room temperature and at 277 K, mixing 0.5 µl of protein and well solution. The reservoir solution volume was 50 µl. *Pf*ADF1 crystals (Fig. 1*a*) formed in 10 d at 277 K in 2.5 *M* ammonium sulfate, 0.1 *M* HEPES pH 7.6–8.0. The crystal used for data collection was grown at pH 7.8. *Pb*ADF2 crystals (Fig. 1*b*) grew overnight at both temperatures in 24–28% polyethylene glycol (PEG) 10 000, 0.1 *M* sodium acetate pH 4.5–5.5. A crystal grown at 277 K in 26% PEG 10 000, 0.1 *M* sodium acetate pH 5.2 was used for data collection.

2.4. Diffraction data collection

Prior to data collection, crystals were flash-frozen in liquid nitrogen without additional cryoprotectants. Because the *Pf*ADF1 crystal suffered on freezing, as was apparent from the smeary diffraction spots and several strong ice rings, annealing by blocking the stream of liquid nitrogen for 10 s was performed to improve the diffraction properties of the crystal. Subsequently, diffraction data sets were collected from single crystals of *Pf*ADF1 and *Pb*ADF2 to 2.0 and 2.1 Å resolution, respectively, using MAR 165 and MAR Mosaic225 CCD detectors mounted on beamlines I911-2 and I911-3 at MAX-Lab, Lund, Sweden. The data were indexed and integrated using *XDS* (Kabsch, 1993) and scaled using *XSCALE* (Kabsch, 1993) using the graphical *XDSi* interface (Kursula, 2004). The complete data-collection statistics are shown in Table 1.

Table 1
Data-collection statistics for *Pf*ADF1 and *Pb*ADF2.

Values in parentheses are for the highest resolution shell.

	*Pf*ADF1	*Pb*ADF2
Beamline	I911-2	I911-3
Wavelength (Å)	1.0380	0.9790
Beam size (mm)	0.3 × 0.3	0.15 × 0.25
Space group	$P3_121/P3_221$	$P2_12_12$
Crystal dimensions (mm)	0.2 × 0.15 × 0.15	0.2 × 0.05 × 0.05
Unit-cell parameters	$a = b = 68.84$, $c = 76.03$, $\alpha = \beta = 90$, $\gamma = 120$	$a = 111.58$, $b = 57.90$, $c = 40.49$, $\alpha = \beta = \gamma = 90$
Resolution range (Å)	20.0–2.0 (2.05–2.0)	20–2.1 (2.15–2.1)
Oscillation per frame (°)	1	0.25
No. of frames collected	180	653
No. of measured reflections	145966 (7050)	97420 (7461)
No. of unique reflections	14010 (1004)	15859 (1168)
Criterion for observed reflections [$I/\sigma(I)$]	−3	−3
Multiplicity	10.4 (7.0)	6.1 (6.4)
Completeness (%)	96.5 (94.5)	99.1 (99.8)
Average $I/\sigma(I)$	38.5 (14.5)	16.4 (4.2)
$R_{\rm merge}$† (%)	4.6 (27.5)	6.0 (64.9)

† $R_{\rm merge} = \sum_{hkl}\sum_i |I_i(hkl) - \langle I(hkl)\rangle| / \sum_{hkl}\sum_i I_i(hkl)$, where $I_i(hkl)$ is the intensity of the *i*th measurement of reflection *hkl* and $\langle I(hkl)\rangle$ is the mean intensity of reflection *hkl*.

3. Results and discussion

*Pf*ADF1 and *Pb*ADF2 were purified using affinity and size-exclusion chromatography. For *Pf*ADF1, an additional ion-exchange chromatography step had to be added between these steps in order to avoid precipitation during concentration before size-exclusion chromatography. A thermal shift assay was used to determine the stability of *Pf*ADF1 in various buffers. The protein was most stable at pH 8.5 or 6.5 with low salt concentrations, such as 50 m*M* NaCl and 0–5% glycerol. The apparent molecular weights of *Pf*ADF1 and *Pb*ADF2 as deduced from SDS–PAGE (Laemmli, 1970) were, as expected, 14 and 17 kDa, respectively, and analytical gel filtration together with static and dynamic light scattering confirmed *Pf*ADF1 to be monomeric in solution (data not shown). The molecular weight of *Pf*ADF1 deduced from static light scattering was 13.5 kDa, which was very close to the calculated molecular weight of 13.7 kDa, and dynamic light scattering showed the protein to be monodisperse. The SRCD data indicated that *Pb*ADF2 was folded and had the expected secondary-structure content of a member of the ADF/cofilin family (data not shown). It could also be seen that *Pb*ADF2 partially loses its secondary structure when stored unfrozen on ice for a period of two weeks.

We determined the solution structures of *Pf*ADF1 and *Pb*ADF2 using SAXS. These structures also show that both proteins are folded and monomeric in solution. It can also be seen that *Pb*ADF2 has a more elongated structure, as expected from the structures of other members of the ADF/cofilin family, whereas *Pf*ADF1 is more spherical (Fig. 2).

Crystallization trials were performed using different protein concentrations and numerous commercially available and homemade crystallization screens both manually and using robotics. Finally, single crystals sufficiently large for diffraction data collection grew in manual sitting-drop vapour-diffusion setups at 277 K. The *Pf*ADF1 crystal belonged to space group $P3_121$ or $P3_221$, with unit-cell parameters $a = b = 68.8$, $c = 76.0$ Å (Table 1). The Matthews coefficient ($V_{\rm M}$; Matthews, 1968) of 3.71 or 1.86 Å^3 Da^{-1} indicated the presence of one or two monomers in the asymmetric unit, with possible solvent contents of 67 or 34%, respectively. The crystal of *Pb*ADF2 belonged

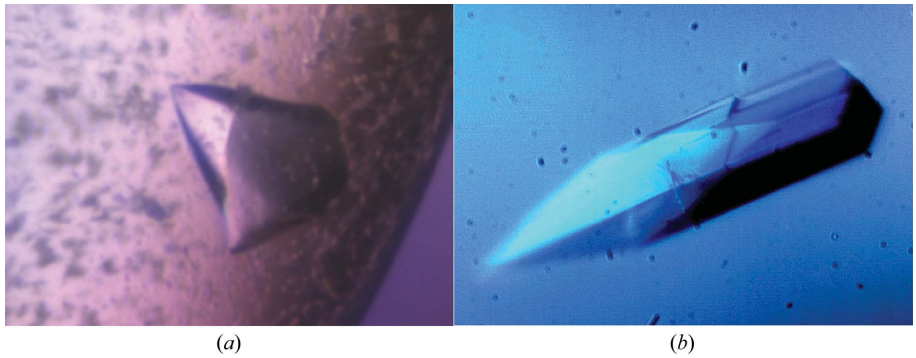

(*a*) (*b*)

Figure 1
(*a*) A single crystal of *Pf*ADF1 grown in 2.5 *M* ammonium sulfate, 0.1 *M* HEPES pH 7.8. (*b*) A single crystal of *Pb*ADF2 grown in 26% PEG 10 000, 0.1 *M* sodium acetate pH 5.2. The maximum dimension of both crystals was approximately 200 µm.

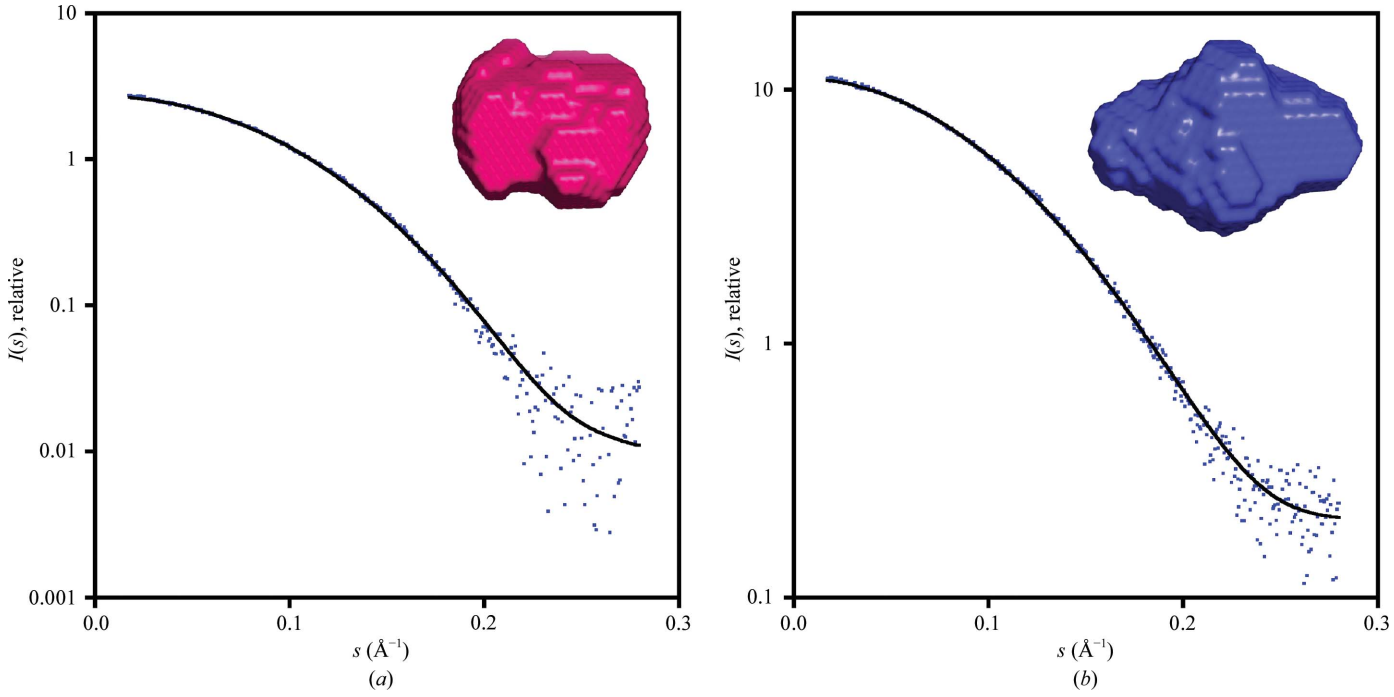

Figure 2
Calculated SAXS envelopes of (*a*) *Pf*ADF1 and (*b*) *Pb*ADF2 and the corresponding X-ray scattering curves. The dots are the measured scattering intensities and the solid line describes the fit of the calculated model to the measured data.

to space group $P2_12_12$, with unit-cell parameters $a = 111.6$, $b = 57.9$, $c = 40.5$ Å (Table 1). The V_M of 4.39 or 2.19 Å^3 Da^{-1} indicated the presence of one or two monomers in the asymmetric unit, with possible solvent contents of 72 or 44%, respectively. The lack of significant peaks above the noise level in addition to the peaks corresponding to the crystallographic symmetry in a self-rotation function calculated using *MOLREP* (Vagin & Teplyakov, 1997) for both data sets indicates either the presence of only one molecule in the asymmetric unit or that a possible noncrystallographic symmetry axis is parallel with one of the crystallographic symmetry axes. As discussed above, both *Pf*ADF1 and *Pb*ADF2 were shown to be monomeric in solution using several methods.

High-resolution diffraction data sets could be collected from both *Pf*ADF1 and *Pb*ADF2 crystals. The data sets could be processed to 2.0 and 2.1 Å resolution, respectively, with good statistics (Table 1). For the *Pf*ADF1 crystal, it seems likely that higher resolution data could possibly be obtained. The *Pf*ADF1 crystal initially suffered on freezing without cryoprotection, but the strong ice rings could be removed and the diffraction limit and the quality of the diffraction spots could be clearly improved by annealing. Structure determination of both apicomplexan ADFs by molecular replacement is ongoing. Several crystal and solution structures of members of the ADF/cofilin family from plants (Bowman *et al.*, 2000), yeast (Andrianantoandro & Pollard, 2006), amoebae (Blanchoin & Pollard, 1998) and mammals (Pope *et al.*, 2004), as well as of complexes with monomeric actin (Paavilainen *et al.*, 2008), are available in the Protein Data Bank. All of these proteins have rather low sequence identity to the apicomplexan ADFs, with the closest homologues sharing about 30% sequence identity. Based on a promising molecular-replacement solution, it seems likely that the correct space group of the *Pf*ADF1 crystal is $P3_221$. From the systematic absences, it is clear that the *Pb*ADF2 crystal belongs to space group $P2_12_12$ and this also seems to be confirmed by the molecular-replacement trials. We expect the crystal structures of *Plasmodium* ADFs to explain the functional differences between ADFs from apicomplexan parasites and higher eukaryotes such as their mammalian hosts.

We would like to thank Matti Myllykoski and Dr Petri Kursula for help with synchrotron data collection and Eeva-Liisa Stefanius and Dr Ulrich Bergmann for skilful assistance with mass spectrometry. The user support at MAX-Lab beamlines I711, I911-2 and I911-3, EMBL-DESY beamline X33 and BESSY beamline 3m-NIM is gratefully acknowledged. This work was financially supported by the Academy of Finland, the European Commission FP7 Marie Curie European reintegration program, the Centre for International Mobility/Sitra and the Sigrid Jusélius Foundation.

References

Andrianantoandro, E. & Pollard, T. D. (2006). *Mol. Cell*, **24**, 13–23.
Bamburg, J. R. (1999). *Annu. Rev. Cell Dev. Biol.* **15**, 185–230.
Bergman, L. W., Kaiser, K., Fujioka, H., Coppens, I., Daly, T. M., Fox, S., Matuschewski, K., Nussenzweig, V. & Kappe, S. H. (2003). *J. Cell Sci.* **116**, 39–49.
Bernstein, B. W. & Bamburg, J. R. (2010). *Trends Cell Biol.* **20**, 187–195.
Blanchoin, L. & Pollard, T. D. (1998). *J. Biol. Chem.* **273**, 25106–25111.
Bowman, G. D., Nodelman, I. M., Hong, Y., Chua, N.-H., Lindberg, U. & Schutt, C. E. (2000). *Proteins*, **41**, 374–384.
Carlier, M.-F., Laurent, V., Santolini, J., Melki, R., Didry, D., Xia, G.-X., Hong, Y., Chua, N.-H. & Pantaloni, D. (1997). *J. Cell Biol.* **136**, 1307–1322.
Ericsson, U. B., Hällberg, B. M., DeTitta, G. T., Dekker, N. & Nordlund, P. (2006). *Anal. Biochem.* **357**, 289–298.
Jewett, T. J. & Sibley, L. D. (2003). *Mol. Cell*, **11**, 885–894.
Kabsch, W. (1993). *J. Appl. Cryst.* **26**, 795–800.
Konarev, P. V., Petoukhov, M. V., Volkov, V. V. & Svergun, D. I. (2006). *J. Appl. Cryst.* **39**, 277–286.
Konarev, P. V., Volkov, V. V., Sokolova, A. V., Koch, M. H. J. & Svergun, D. I. (2003). *J. Appl. Cryst.* **36**, 1277–1282.
Kursula, P. (2004). *J. Appl. Cryst.* **37**, 347–348.
Laemmli, U. K. (1970). *Nature (London)*, **227**, 680–685.

Majava, V., Wang, C., Myllykoski, M., Kangas, S. M., Kang, S. U., Hayashi, N., Baumgärtel, P., Heape, A. M., Lubec, G. & Kursula, P. (2009). *Amino Acids*, doi:10.1007/s00726-009-0364-2.
Matthews, B. W. (1968). *J. Mol. Biol.* **33**, 491–497.
Mehta, S. & Sibley, L. D. (2010). *J. Biol. Chem.* **285**, 6835–6847.
Paavilainen, V. O., Oksanen, E., Goldman, A. & Lappalainen, P. (2008). *J. Cell. Biol.* **182**, 51–59.
Pope, B. J., Zierler-Gould, K. M., Kuhne, R., Weeds, A. G. & Ball, L. J. (2004). *J. Biol. Chem.* **279**, 4840–4848.
Schatten, H., Sibley, L. D. & Ris, H. (2003). *Microsc. Microanal.* **9**, 330–335.
Schmitz, S., Grainger, M., Howell, S., Calder, L. J., Gaeb, M., Pinder, J. C., Holder, A. A. & Veigel, C. (2005). *J. Mol. Biol.* **349**, 113–125.
Schüler, H. & Matuschewski, K. (2006). *Traffic*, **7**, 1433–1439.
Schüler, H., Mueller, A. K. & Matuschewski, K. (2005). *Mol. Biol. Cell*, **16**, 4013–4023.
Sibley, L. D. (2004). *Science*, **304**, 248–253.
Studier, F. W. (2005). *Protein Expr. Purif.* **41**, 207–234.
Svergun, D. I. (1992). *J. Appl. Cryst.* **25**, 495–503.
Svergun, D. I. (1999). *Biophys. J.* **76**, 2879–2886.
Troys, M. van, Huyck, L., Leyman, S., Dhaese, S., Vandekerkhove, J. & Ampe, C. (2008). *Eur. J. Cell Biol.* **87**, 649–667.
Vagin, A. & Teplyakov, A. (1997). *J. Appl. Cryst.* **30**, 1022–1025.
Volkov, V. V. & Svergun, D. I. (2003). *J. Appl. Cryst.* **36**, 860–864.